RSC Advances

ROYAL SOCIETY OF CHEMISTRY

www.rsc.org/advances

Journal Name

ARTICLE

Fabrication of Cationized Gelatin Nanofibers by Electrospinning for Tissue Regeneration

Received 00th January 20xx,
Accepted 00th January 20xx

DOI: 10.1039/x0xx00000x

www.rsc.org/

Jalaja K[a], Deboki Naskar[b], Subhas C Kundu[b] and Nirmala Rachel James[a*]

Gelatin based electrospun nanofibers are promising candidates for tissue engineering and regenerative medicine due to their properties like biocompatibility, non antigenicity, non-toxicity and structural resemblance with native extracellular matrix. In the present work, a new nanofibrous scaffold using amine functionalized gelatin is fabricated. Modified gelatin is also known by the name cationized gelatin as the amino group is getting protonated. Unlike gelatin, the cationized gelatin is soluble in water without forming gel at room temperature. Hence, electrospinning of cationized gelatin can be carried out using water as the solvent. The water stability of cationized gelatin nanofibers is improved by cross-linking with two novel cross-linking agents, namely a disaccharide (sucrose) and a polysaccharide (dextran). The resulting cationized gelatin nanofibers are evaluated for the mouse fibroblast and human osteoblast like cells attachment, adhesion and proliferation. The results demonstrate that the electrospun cationized gelatin nanofibers can be potential scaffold materials for tissue regenerations.

Introduction

Gelatin is a natural polymer derived from collagen, commonly applied for pharmaceutical and medical purposes due to the wealth of merits such as biological origin, non-immunogenicity, biodegradability and biocompatibility[1]. Gelatin nanofibers exhibit the special properties in conjunction with enhanced surface area and functionality, making them suitable in the development of bio mimicking artificial extracellular matrix, wound dressing materials with antibacterial properties and drug delivery matrices[2, 3]. Gelatin nanofibers are fabricated by an attractive technique known as electrospinning[4]. The ultrafine fibers can be produced by electrospinning method using a wide variety of materials such as polymers, ceramics and metals. The fabrication of gelatin nanofibers by electrospinning requires toxic organic solvents such as trifluoro ethanol (TFE)[5], hexafluoro isopropanol (HFIP)[6], formic acid[7], acetic acid[8] and others. These solvents if left in the nanostructures can be toxic to the living tissues[9]. The resultant nanofibers are cross-linked using bifunctional cross-linkers such as glutaraldehyde[10], isocyanates[11], acyl azides[12] and others in order to improve their water stability. These cross-linkers are shown to be toxic, if released into the body due to degradation or left unreacted in the fibrous structures[10, 13]. Genipin, a natural molecule, which is less toxic than glutaraldehyde is reported to be an effective cross-linker for gelatin based nanofibers[14]. However, the high cost of the genipin makes it out of place for real life applications. The researchers in the field of biomedical nanofibers are trying hard to avoid or reduce the toxicity in gelatin and other protein based nanofibers either by using alternative solvent system or by using novel cross-linkers. The fabrication of gelatin nanofibers using 8:2 v/v water / acetic acid solvent mixture followed by cross-linking of the nanofibers by naturally derived cross-linking agents based on dextran[15] and sucrose[16] is reported by us recently. The present study also aims at improvement of the performance of gelatin nanofibers by introducing excess amino groups on gelatin.

Gelatin contains 18 distinct amino acids with both positive and negative charges, which are distributed non-uniformly[17]. Gelatin is obtained by acidic or alkaline treatment of collagen resulting in gelatin type A (isoelectric point from 7–9.5) and gelatin type B (isoelectric point from 4.5–5.3) respectively[18, 19]. The alkaline process hydrolyses the amide groups into carboxyl groups, resulting in gelatin type B with a higher density of carboxyl groups, making it negatively charged and lowering its isoelectric point[19]. In contrast, acidic pre-treatment does not significantly affect the amide groups and results in gelatin type A with more number of amino groups[20]. Gelatin shows inherent cationic property due to the basic amino acid residues such as arginine and lysine. The amino groups get protonated at pH values less than the isoelectric point. Gelatin can also be cationized by introducing amino groups onto the gelatin backbone, usually realized by carbodiimide chemistry. Cationic gelatin is obtained by coupling ethylenediamine or spermine through a carbodiimide mediated reaction[21]. Gelatin

[a] Department of Chemistry, Indian Institute of Space Science and Technology, Thiruvananthapuram- 695 547, India.
[b] Department of Biotechnology, Indian Institute of Technology Kharagpur, West Bengal - 721302, India

Electronic Supplementary Information (ESI) available: [Cross-linking CG nanofibers using glutaraldehyde, SEM images of GT-CG, MTT assay of L-929 cells cultured on DA-CG, SA-CG and GT-CG nanofibers]. See DOI: 10.1039/x0xx00000x

is usually cationically modified to facilitate the interactions with biomolecules of anionic nature[21, 22]. Anchorage of excess amino groups on gelatin surface provides a suitable way to enhance the cell affinity of biomaterials.

In the present research work, type A gelatin is cationized by ethylene diamine and 1-ethyl, 3-[3 dimethyl aminopropyl] carbodiimide (EDC). Several reports on cationized gelatin matrices are available for drug and gene delivery[23, 24] . A few reports are also found on the tissue regeneration using cationic gelatin as a coating over synthetic polymers[25, 26]. The core shell nanofibers are fabricated using polycaprolactum (PCL) as core and cationized gelatin (CG) as shell material using trifluoro ethanol (TFE) as solvent[27]. Cationized gelatin as shell material enables a bio compatible surface. This allows the immobilization of negatively charged bioactive molecules, and facilitates the cell adhesion and proliferation[27]. We envision that pure CG nanofibers can act as a better bio compatible material for tissue regeneration. It is observed that the CG is highly soluble in water without forming gel at room temperature. Hence, water is selected as the solvent for CG nanofiber production. It replaces all other toxic solvents such as TFE, HFIP, formic acid and acetic acid, which are being conventionally employed. This method will greatly assist the efforts of the researchers to reduce the toxicity due to the presence of solvents in the case of protein nanofibers. Also, the cationic surface of the nanofibers will enable a better interaction with the anionic cell surface, which may promote greater cell attachment and proliferation. Since CG is highly hydrophilic in nature, cross-linking treatment is necessary to improve the water resistance of nanofibers for tissue regeneration applicability. The external cross-linkers are reported to be a common source of toxicity in a biodegradable material. The biocompatibility and non-toxicity of dextran aldehyde and sucrose aldehyde cross-linkers with gelatin nanofibers are already established in our earlier works[15, 16]. Hence, the fabricated nanofibers in the present work are cross-linked using dextran aldehyde (DA) and sucrose aldehyde (SA).

This is the first report on fabricating electrospun CG nanofibers using pure water as the solvent. We employ dextran aldehyde (DA) and sucrose aldehyde (SA) as cross-linking agents to avoid any toxicity to the CG nanofibers. The results indicate that, this novel way of nanofiber fabrication is a promising approach for tissue regeneration applications.

Materials and methods

Materials

Type A gelatin from porcine skin (225 bloom), trinitrobenzene sulfonic acid (TNBS) (1 % w/v solution), dextran from Leuconostocmesenteroids, beta alanine (Sigma Aldrich, Saint Louis, USA), 1-ethyl,3-[3 dimethyl aminopropyl] carbodiimide (EDC) (Spectrochem PVT Ltd, Mumbai), ethylenediamine (EDA), disodium hydrogen phosphate, sodium dihydrogenphosphate, sodium chloride, sucrose (Merck, Mumbai, India), dialysis tubing with MWCO 6000 (Spectrum Laboratories Inc.CA, USA), Alamar blue dye and Alexa Fluor 594 and Hoechst 33258 dyes (Invitrogen, Thermo Fisher Scientific, USA) were used as received.

Preparation of cationized gelatin (CG)

Cationized gelatin was prepared by chemically converting carboxyl groups of gelatin into amino groups according to Shen et al [26]. Briefly, 15.1 ml of EDA was added into 200 ml of 0.1 M phosphate-buffered saline (PBS, pH = 5.0) containing 5 g of gelatin. The pH of the solution was adjusted to 5.0 by adding 5 M HCl immediately. EDC (5. 35 g) was added to this solution, which was made up to 250 ml with PBS. The reaction mixture was agitated at room temperature for 18-20 h and then dialyzed against double distilled water for 3 days. The dialyzed solution was freeze-dried to obtain cationized gelatin.

Electrospinning of CG

Electrospinning was performed using a horizontal set up containing a variable high DC voltage power supply and a programmable syringe pump (ESPIN NANO, Physics Instrument Company, Chennai). Different weight percent of CG was prepared in water (30 - 50 % (w/v)) and were poured into 5 ml plastic syringes mounted on the pump. Fiber mats were collected on an aluminium foil attached to a drum collector that could easily be removed for subsequent characterization. An in-house designed drum with both rotational and translational controllable movements was connected to the power supply, 15 cm away from the needle. Samples were collected in rotating drum mode. Flow rates of 0.2−0.3 ml/h and a voltage range of 25−30 kV was used as process parameters. The electrospinning parameters used were chosen based on trial and error optimization procedure.

Cross-linking of cationized gelatin nanofibers

Nanofibrous matrices fabricated from CG are found to be highly soluble and hence the water stability of CG nanofibers has to be improved by effective cross-linking approaches. Two novel cross-linking agents for CG nanofibers based on natural and non-toxic materials, namely dextran and sucrose in their oxidized forms are introduced. Dextran aldehyde (DA) was prepared by periodate oxidation according to Domb et al[28]. In brief, 2.66 g of $NaIO_4$ was dissolved in 10 ml of water containing 1 g of dextran and the reaction mixture was stirred under dark for 6 h at 25 $^{\circ}$C. The resulting solution was dialyzed against double distilled water for 3 days by changing water until it was free from periodate. Samples were frosted by keeping at -20 $^{\circ}$C and thereafter dried by lyophilization. DA (0.05 g) was dissolved in 10 ml of ethanol containing a minimum quantity of aqueous borax (300 µl, 0.02 M borax solution). About 0.5 g of the electrospun CG mats were cut into rectangular pieces and placed in this cross-linking medium for 7 days at 37 $^{\circ}$C to obtain DA cross-linked CG nanofibers (DA-CG).

Periodate oxidation of sucrose was carried out according to Rob Schoevaart et al with slight modification [29]. In brief, 3.42 g (0.01 mol) sucrose was dissolved in 50 ml of water and to this 4.26 g (0.02 mol) of $NaIO_4$ was added. After stirring the reaction mixture in dark for 6 h, excess amount of acetone was

added and the mixture was cooled on ice. Filtration and evaporation of the acetone yielded a 50 ml solution of the sucrose aldehyde (SA) cross-linker. The resulting solution was kept in deep freezer at -20 °C and thereafter dried by lyophilization to get oxidized sucrose in powder form. Sucrose aldehyde (0.1 g) was dissolved in 10 ml of pure ethanol and cross-linked CG mats were prepared by dipping around 0.5 g of CG nanofibrous mats in the ethanolic solution of SA for 7 days at 37 °C to obtain SA cross-linked CG nanofibers (SA-CG).

Biophysical characterizations

Fourier transform infrared (FTIR) analysis: Fourier transform infrared (FTIR) spectra of gelatin, CG and cross-linked CG nanofibers were obtained (Spectrum 100, Perkin Elmer) with universal attenuated total reflectance accessory (UATR) using standard ZnSe crystal. For each spectrum, 32 scans were accumulated at 4 cm^{-1} resolution in the scanning range of 4000-650 cm^{-1}.

Thermal characterizations: Thermogravimetric analysis (TGA) of gelatin, CG and CG nanofibers was carried out in nitrogen atmosphere using a thermo gravimetric analyzer (Q-50, TA instruments, USA). The heating rate used was 10 °C/min from room temperature to 500 °C. Differential scanning calorimetry (DSC) of the samples was performed (Q-20, TA instruments, USA) at a heating rate of 10 °C/min from -20 °C to 280 °C.

Trinitro benzene sulfonic acid (TNBS) assay: The amino groups introduced onto gelatin after cationization was determined by the conventional TNBS assay based on the calibration curve prepared by β-alanine. Briefly, 2 mg each of gelatin and cationized gelatin samples were added to 1 ml of 4 % sodium bicarbonate and 0.1 % freshly prepared TNBS solution. After thorough mixing, the solutions were placed in water bath at 40 °C for 2 h. For complete dissolution of the samples, 3 ml of 6 N HCl was added and temperature was raised to 60 °C and heated for 1 h. Blank solutions were prepared using the same procedure without the test samples. Absorbance values of the solutions were then determined spectrophotometrically (at 346 nm; UV-Visible Spectrophotometer, Cary win UV). From the β-alanine calibration curve prepared using the same method, amino groups of gelatin and cationized gelatin can be quantified.

The absorbance values of as spun and cross-linked CG mats also were evaluated by the same method. The degree of cross-linking of the cross-linked CG nanofibers was determined as follows.

Degree of cross-linking = $1-\{(\text{absorbance}_{cl}/\text{mass}_{cl}) \times (\text{absorbance}_{ucl}/\text{mass}_{ucl})^{-1}\}$

The subscripts cl and ucl stand for the cross-linked and uncross-linked CG nanofibers.

Zeta potential: Zeta potential of gelatin and CG samples were determined at 1 % (w/v) concentration in PBS using Zetasizer, Malvern Instrument Ltd.

X-ray diffraction (XRD) analysis: X-ray diffraction analysis of gelatin and CG samples was carried out using Bruker D 8 discover small angle X-ray diffractometer with 2θ ranging from 10 ° to 90 °.

X-ray Photoelectron spectroscopy (XPS): Surface characteristics and atomic composition of gelatin and CG were obtained from X-ray photo electron spectroscopic (XPS) analysis using Omicron ESCA probe spectrometer with X-ray source of polychromatic Mg Kα.

Rheological behavior of gelatin and CG: Rheological behavior of aqueous solutions of gelatin and CG were analyzed by means of rheometer (Antopaar) by varying the shear rate and temperature.

Scanning electron microscopy (SEM): A scanning electron microscope operating at 20 kV and 10 μA was used to analyze the morphology and size of the nanofibers (FEI- Quanta, FE-SEM). All the samples were mounted using carbon tape on aluminium SEM stubs after gold sputtering. The diameter histogram of the mats was recorded from SEM image using imageJ software for 200 data points.

Swelling and degradation behavior: The water stability of cross-linked CG nanofibers was examined in terms of their swelling characteristics. This swelling ratio also gives direct evidence for the extent of cross-linking of CG with the cross-linking agents. Swelling of as spun and the cross-linked mats were carried out by dipping the previously weighed mats in PBS (pH 7.4) at 37 °C for different time periods. From the dry and swollen weights of the samples, the swelling ratio was calculated using the following formula:

Swelling ratio (%) = $((W_s - W_d) / W_d) \times 100$

(Where W_d and W_s are the weights of the samples in the dry and swollen states, respectively).

In vitro degradation studies of the cross-linked CG nanofibers were performed in PBS at 37 °C. Previously weighed and dried samples (1 cm^2, n=3) were immersed in 2 ml of PBS for a time period of 6 weeks. Experiment was performed in aseptic conditions. After the predetermined time, medium was removed and weights of the samples were measured after lyophilization.

Weight ratio= W_2/W_1

W_1 and W_2 are the initial and final weights of the samples.

Mechanical behaviour: The cross-linked and uncross-linked CG nanofibers are examined for their mechanical behaviour via tensile stress – strain experiment using Universal testing Machine (Instron 5050, Instron USA) with a load cell of 100 N capacity. Specimens were cut in the form of rectangular strips (5 × 0.4 cm^2) with an average thickness of 0.2 mm, and tested at a crosshead speed of 10 mm/min. Stress at break and Young's modulus were measured based on stress-strain curve.

Cell culture

Cell culture and maintenance: Mouse subcutaneous fibroblasts (L-929 cell line, National Centre For Cell Science, Pune)and Human osteoblast like cell line (MG 63, National Centre For Cell Science, Pune) were maintained in Dulbecco's Modified Eagle's Medium (DMEM) (Gibco BRL Grand Island, NY, USA) supplemented with 10 % Foetal Bovine Serum, 100 U/ml Penicillin and 100 µg/ml Streptomycin (Gibco BRL Grand Island, NY, USA) in a CO_2 incubator (Heracell, Thermo Scientific) set at 37 °C, 5 % CO_2 and >90 % relative humidity. The cells were detached using 0.05 % Trypsin EDTA (Himedia, India) solution, centrifuged, counted using hemocytometer and desired number of cells were used for seeding.

Preparation of matrices before cell culture and cell seeding: The mats were cut into 1cm ×1cm pieces and kept in each well of 24 well sterile tissue culture plates. The mats were sterilized by immersing in 100 % ethanol followed by exposure in Ultra Violet light. After sterilization, the mats were washed thoroughly using sterile PBS 3 times for 15 min each. Finally the mats were soaked in DMEM medium for 1 h for conditioning before cell seeding. Desired number of cells (2000 cells) were seeded on each conditioned mat and allowed to adhere and grow on DA-CG and SA-CG mats. Cells cultured on cover glass were considered as control.

Adhesion of L-929 and MG-63 cells: The cell adhesion was analyzed by visualizing the morphology of adhered cells by staining the actin cytoskeleton structures. After the stipulated time period, L-929 and MG-63 cells were fixed (48 h and 5th day respectively) using 4 % paraformaldehyde for 1 h at room temperature and rinsed with PBS. The cell membrane was permeabilized by treating with 0.1 % Triton-X 100 for 5 min and actin filaments were stained by incubating the samples with rhodamine - phalloidin (1:500 dilutions in PBS) for 1 h. The cell nucleus was counter stained using Hoechst 33258 dye (1:600 dilutions in PBS) by incubating the samples with the dye for 5 min. The cell adhesion was observed under confocal laser scanning microscope (Olympus Fluo View FV 1000) using 405 nm laser for Hoechst and 543 nm laser for rhodamine - phalloidin.

Proliferation and viability of MG-63 cells: The proliferation of osteoblast cells at different day points on the mats were investigated using Alamar blue assay. The cell seeded mats were transferred to a new 24 well tissue culture plate aseptically. On the desired day point (day 1, day 3, day 5 and day 7), the spent supernatant medium was removed and Alamar blue solution (diluted 1:10 in incomplete DMEM medium) was added to the mats following manufacturers' protocol. The plates were incubated in CO_2 incubator for 4 h in dark condition. After incubation, the supernatant medium was collected in a new 96 well flat bottom tissue culture plate and fresh medium was added in each mat allowing the cells to grow. The reduction of dye was measured photometrically using 570 nm and 600 nm filters of a microplate reader (Thermo Scientific Multiskan Spectrum, Japan).

The cell viability and proliferation were investigated using live dead assay. The cell seeded mats were collected at 5th day of seeding and washed with sterile PBS. The mats were then incubated with Live/Dead stain (Molecular Probes, Invitrogen, USA) for 30 mins inside the CO_2 incubator. The mats were then visualized using confocal laser scanning microscope (Olympus Fluo View FV 1000). Laser of 488 nm was used for imaging the live cells (calcein AM) and 543 nm laser was used for imaging the dead cells (ethidiumhomodimer).

Statistical analysis: Statistical analysis for the determination of difference in means among the groups was accomplished by one way ANOVA (using Origin Pro 8.5 software). At least 8 replications were analysed from each sample of each day point. The symbol '***' denotes statistically significant difference among the groups at alpha value 0.001. All data are presented as mean value with standard errors (mean±SE).

Results and Discussion

Characterization of CG

Gelatin can be cationically modified to augment interactions with biomolecules and cell membranes, which are anionic in nature. It is reported that the surface of poly-L-glycolic acid (PLGA) and poly-L-lactic acid (PLLA) films and sponges when modified with CG show enhanced cell attachment and growth of mouse NIH 3T3 fibroblasts cells and articular chondrocytes cells, respectively, in comparison with gelatin[25, 26]. The large number of positive charges on the surface of CG would enable a better interaction with the negatively charged cell surface. This can provide an excellent cellular adhesion and proliferation. In the present work, novel gelatin based nanofibers are fabricated from cationically modified gelatin. The purpose of the study is not only to minimize the toxicity effects from solvents and cross-linking agents, but also to improve the cell attachment and growth on the nanofibrous substrate. Cationic modification of gelatin is accomplished by introducing amino groups onto the gelatin backbone through carbodiimide mediated reaction. This reaction establishes amide bonds between carboxylic groups of gelatin and amino groups of ethylenediamine as shown in Figure 1.

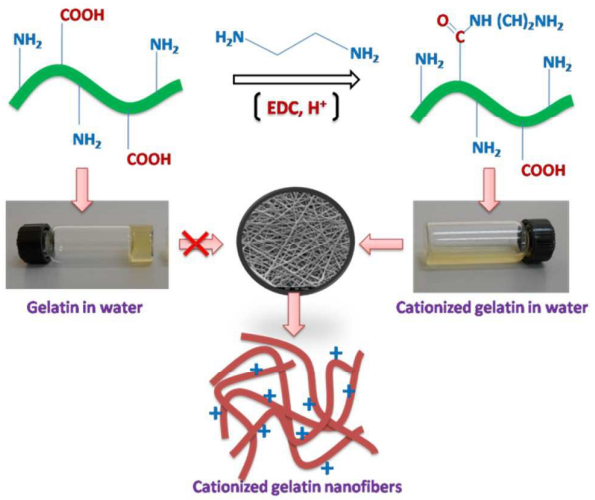

Figure 1: Schematic for CG formation and nanofiber fabrication from aqueous solution

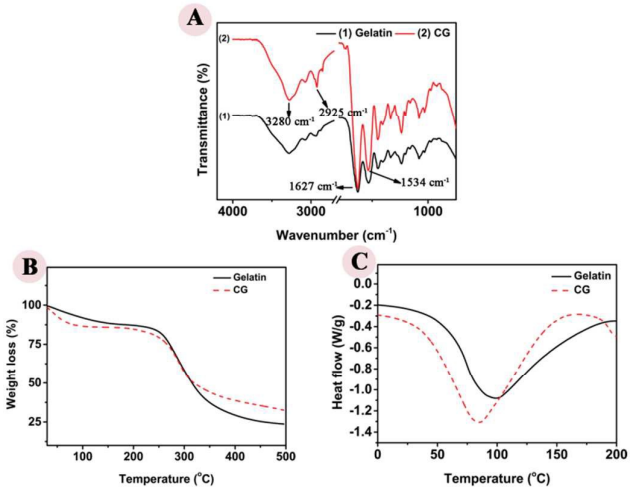

Figure 2: (A) FT-IR spectra, (B) TGA and (C) DSC thermograms of gelatin and cationized gelatin

FT-IR spectra of gelatin and CG are shown in Figure 2 (A). The spectrum of gelatin contains a broad band at 3280 cm^{-1} due to –OH and –NH stretching. Bands at 1627 and 1534 are assigned to amide I and amide II bands, respectively. Other than the peaks from gelatin, the IR spectrum of CG shows an additional peak at 2925 cm^{-1} associated with the C-H stretching from ethylenediamine groups.

Thermal analysis of gelatin and CG is carried out in order to know the effect of cationization on thermal behaviour of gelatin. TGA thermograms of gelatin and CG are shown in Figure 2 (B). CG shows similar thermal degradation pattern as that of gelatin, but with higher char residue. In the TGA thermogram, it can be seen that as a result of incorporation of large number of ethylenediamine groups, there is an increase in the carbon yield for CG (29 %) compared to gelatin (23 %) at 500 ^{o}C. The DSC thermogram (Figure 2 (C)) shows endotherm corresponding to the denaturation temperature of gelatin. The DSC thermogram exhibits lower denaturation temperature for CG than gelatin. During the preparation process of CG, the rupture of triple helix of gelatin takes place, which lowers the thermal stability of CG and hence the endotherm is shifted to a lower temperature compared to gelatin (from 97 to 84 °C).

The excess amino groups introduced on gelatin as a result of cationization are determined by TNBS assay. The number of amino groups in gelatin and CG are 2.2 × 10^{-4} and 4.75 × 10^{-4} mol/g, respectively. The molar ratio of amino groups on CG to that on gelatin is found to be 2.16, close to the value reported in the literature[25]. The zeta potential of CG is determined to find out the surface positive charge. An increase or reduction in zeta potential value is a measure of the presence of charges on the dissociated surface functional groups. In case of gelatin, the negatively charged groups such as carboxylic acid cause decrease of zeta, whereas the positively charged groups such as amino groups enhance the zeta potential value. In comparison with gelatin (-2.1 mV), CG exhibits a more positive zeta potential value of +2.9 mV and indicates the formation of CG.

In order to understand the structural property and surface composition of CG, XRD and XPS analyses are carried out. Gelatin shows a wide crystalline XRD peak at 2θ = 20.9° due to the triple-helical crystalline structure of collagen renatured in gelatin. This peak is absent in the pattern of CG (Figure 3 (A)) indicating the amorphous nature of CG. It is seen from the XRD pattern that, the intensity of the wide crystalline peak at 2θ = 20.9° observed in the pattern of gelatin is considerably reduced in the case of CG, indicating the destruction of the triple helical structure as a result of cationization. This may be due to the reduced extent of hydrogen bonding in the CG as a result of protonation of primary amino groups. XPS survey scan spectra of gelatin and CG are shown in Figure 3 (B). The results clearly reveal that, the N1s peak intensity increases as a result of cationization, which also supports the other observations. From the high resolution C1s, N1s and O1s spectra, the relative atomic percentages are calculated and are summarized in Table 1. From the elemental composition of gelatin and CG obtained from XPS spectra, it is clear that the N1s peak intensity increases as a consequence of cationization.

These data also well-support the presence of large number of amino groups on the surface of CG.

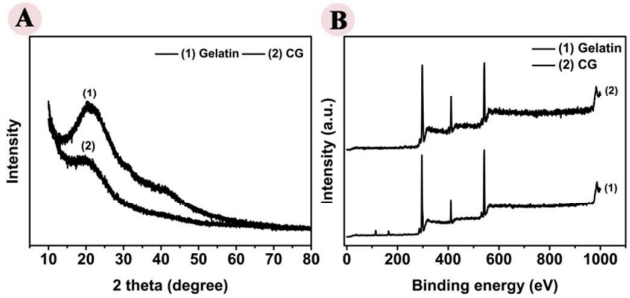

Figure 3: (A) XRD patterns and (B) XPS survey scan spectra of gelatin and cationized gelatin

Table:1 Elemental composition of gelatin and CG from high resolution XPS spectra

Element	CG	Gelatin
C (%)	60.5	67
N (%)	18.5	11.5
O (%)	21	21.5

The rheological behaviour of gelatin and CG in aqueous solution is examined. Figure 4 (B) shows the viscosity values of gelatin and CG solutions (20 % w/v) at 25 and 37 °C. The values are recorded at a shear rate of 100 s^{-1}.The rheological behaviour of aqueous solution of gelatin and CG shows that, after cationization, the viscosity is reduced drastically (Figure 4 (A) and Figure 4 (B)). This is mainly due to the rupture of the triple helical structure of gelatin leading to the reduction in the extent of hydrogen bonding interactions. The higher viscosity value of aqueous gelatin at 25 °C is due to the gelation, as a result of the formation of inter and intramolecular hydrogen bonding among gelatin molecules. When temperature increases to 37 °C, hydrogen bonding breaks and viscosity is drastically reduced. On the other hand, CG shows very low viscosity at 25 °C, compared to gelatin. This is due to the destruction of triple helical structure and loss of hydrogen bonding as a result of cationization. The amino groups are protonated and hence they are not available for hydrogen bonding. Even at 37 °C, there is not much variation in the viscosity of CG solution compared to that at 25 °C. These data obviously provide the evidence for the formation of CG and its solubility in water without undergoing gelation.

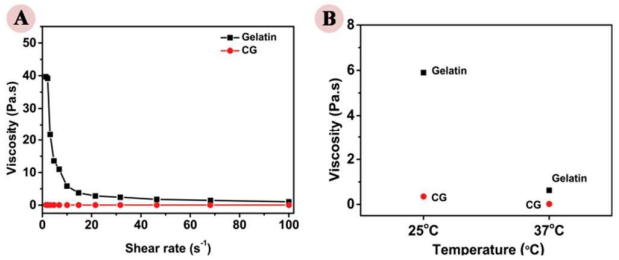

Figure 4: Variation of viscosity with (A) shear rate and (B) temperature for aqueous solutions(20 % w/v)of gelatin and cationized gelatin

Electrospinning of CG

For circumventing the limitations associated with solvents for electrospinning, gelatin is modified by cationization. CG prepared in the present work shows excellent water solubility without forming gel, as is the case with gelatin. This characteristic is clear from Figure 5, which shows the photographs of 20 % aqueous solutions of gelatin and CG taken in sample vials at room temperature. This can aid processing of the material for different applications. This observation throws light towards a novel fabrication strategy for CG nanofibers by electrospinning using water as the solvent.

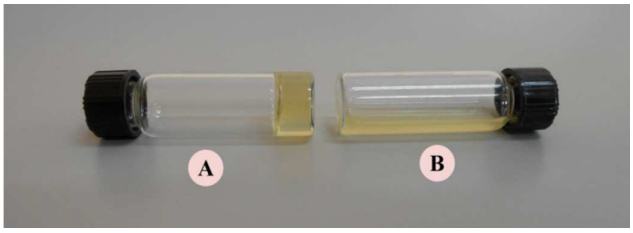

Figure 5: (A) gelatin (20 % w/v) in water and (B) cationized gelatin (20 % w/v) in water at room temperature

Electrospinning of CG is performed by varying the solution and spinning parameters in a trial and error method. The concentrations of CG are varied from 30 to 50 % (w/v). Fibers start forming when CG concentration is 45 % (w/v) and beadless smooth fibers are collected when CG concentration is 50 % (w/v) in water with flow rate of 0.2 ml/h, potential of 25-30 kV and working distance of 15 cm. The nanofibers collected are dried under vacuum and analysed for morphology. SEM image of the CG nanofibers fabricated from pure water at room temperature is shown in Figure 6 (A). The fiber diameter distribution is obtained by measuring the width of 200 individual nanofibers from the SEM image (Figure 6 (B)). The fiber diameter is found to be 130 ± 40 nm.

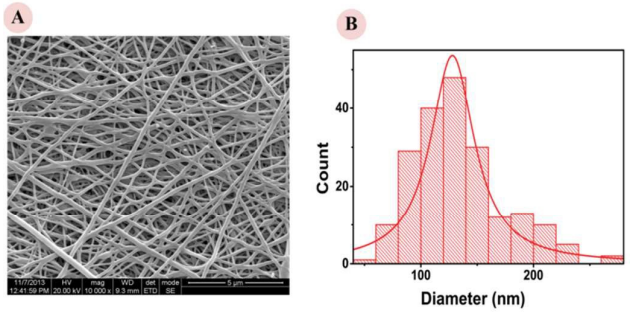

Figure 6: (A) SEM micrograph of electrospun cationized gelatin nanofibers and (B) diameter histogram of cationized gelatin nanofibers

Cross-linking and characterizations of CG nanofibers

CG nanofibers are cross-linked using dextran aldehyde (DA) and sucrose aldehyde (SA). Cross-linking is carried out by dipping the CG nanofibrous mats in ethanol solution of DA and

SA for 7 days. The resulting nanofibers are represented as DA-CG and SA-CG respectively, for cross-linking with DA and SA. The large number of amino groups introduced on gelatin as a result of cationization enable effective cross-linking between amino groups on CG and aldehyde groups on the cross-linking agent by Schiff's base formation. Cross-linking is confirmed by observing the SEM images of cross-linked and swelled mats (Figure 7 (A-D)). SEM images reveal that, cross-linking and subsequent swelling process cause the fibers to lose its discreteness with increase in fiber diameter. However, compared to as spun CG mats, cross-linked mats maintain the fibrous morphology even after dipped in water. The mats are found to be stable in water up to one week without affecting its structural integrity.Thus DA and SA are effective cross-linking agents for CG nanofibers.

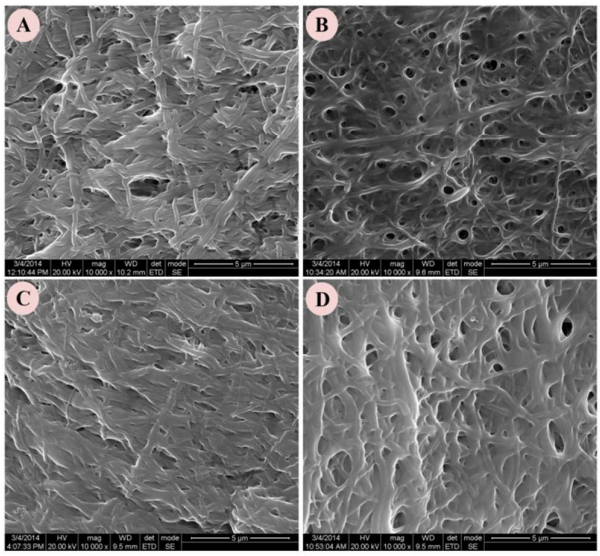

Figure 7: SEM micrographs of (A) dextran aldehyde - cationized gelatin (DA-CG) mats (B) DA-CG swelled mats (C) sucrose aldehyde- cationized gelatin (SA-CG) mats and (D) SA-CG swelled mats. (Mats (B &D) were swelled in water for 24 h)

Cross-linking can be further explained from FTIR spectra and thermograms of the cross-linked mats. FTIR spectra of DA-CG and SA-CG mats show peaks at 1016 cm^{-1} due to the C-O-C stretching frequencies of dextran and sucrose moieties, which is absent in the spectra of as spun CG mat (Figure 8 (A)). DSC thermograms of as spun and cross-linked CG nanofibers are shown in Figure 8 (B). DSC thermogram of as spun CG nanofibers shows endothermic peak at 84 ^{o}C. The cross-linked nanofiber mats show the endothermic peaks at higher temperature regions (DA-CG; 98 ^{o}C, SA-CG; 99 ^{o}C) due to the newly introduced covalent bonds as a result of cross-linking. These results reveal improved thermal stability of DA-CG and SA-CG nanofibrous mats.

Swelling ability of the nanofibrous scaffold helps in maintaining the shape of the scaffold and supports the growth of the cells. Here, as spun CG nanofibers dissolve in water while the cross-linked mats show a stable swelling behaviour. The results of swelling experiment (Figure 8 (C)) show that DA cross-linked mats exhibit a lower swelling ratio which is direct evidence of better cross-linking efficiency of DA compared to SA. Higher degree of cross-linking is due to the macromolecular chain entanglement in DA molecule which causes a better interaction among the chains of DA and gelatin. Also, the presence of small amount of borax in DA solution facilitates the cross-linking. Alkaline pH has an important role in determining the degree of cross-linking between amino groups of gelatin and aldehyde groups of the cross-linking agent. The presence of small amount of water also favours better interaction between CG nanofibers and the cross-linking agent. Sucrose aldehyde also is reported to be an effective cross-linker for proteins, but in this case, SA is dissolved in pure ethanol and thus the interaction between the reactants is less effective. These results further validate the degree of cross-linking obtained from TNBS assay. Table 2 shows the degree of cross-linking of CG mats. From the table, it is clear that DA-CG exhibits higher cross-linking degree compared to SA-CG.

Table 2: Cross-linking degrees of cross-linked CG mats

Cross-linking agent	Degree of cross-linking (%)
Dextran aldehyde (DA)	76 ± 3
Sucrose aldehyde (SA)	60 ± 4

In vitro degradation behaviour of the cross-linked CG nanofibers as a function of degradation time is presented in Figure 8 (D). The rate of weight loss is less in the case of DA-CG in comparison with SA-CG indicating that degradation pattern is affected by the cross-linking degree and the nature of the cross-linker. Cross-linked mats are stable up to one week and there after the mats undergo gradual degradation indicated by the decrease in weights with time. The higher degree of cross-linking in the case of DA-CG results in more resistance to degradation in PBS medium at 37 °C as compared to SA-CG. Similar reports are available in literature explaining the effect of cross-linking degree on the degradation behaviour of the proteins[30]. The presence of covalent bonds formed as a result of cross-linking provides strength for the sample for a longer period during degradation. In the case of cross-linked mats with higher cross-linking degree, more chains have to be cleaved in order to dissolve a fragment in the medium[31].

Nanofibers based on gelatin possess poor mechanical property. This is generally improved by suitable cross-linking treatment. The stress-strain behaviour of as spun and cross-linked CG nanofiber mats are represented in Figure 9 (A) and (B) respectively. The tensile strength of CG nanofiber mat is 7.26 ±0.8 MPa with a Young's modulus of 560±60 MPa. After cross-linking with DA and SA, the CG nanofibers exhibit improvement in the mechanical properties. DA-CG mats possess tensile strength of 30.5 ± 3 MPa and Young's modulus of 1110 ± 70 MPa. The SA-CG mats exhibit tensile strength and Young's modulus of 35.5 ± 2.6 MPa and 950 ±30 MPa respectively. Uncross-linked CG mats have very low tensile strength and the elongation at break. After cross-linking treatments, dramatic change in the tensile strength, modulus

and elongation at break are observed. This result indicates that DA and SA can effectively cross-link CG nanofibers. The mechanical property and degradation behaviour can be tuned for the specific tissue engineering applications by varying the cross-linking conditions.

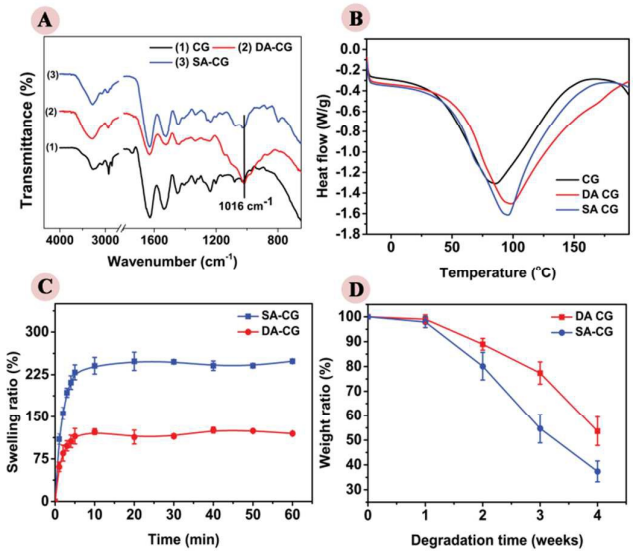

Figure 8: (A) FT-IR spectra, (B) DSC thermograms, (C) swelling behavior and (D) degradation under physiological pH at 37 °C of dextran aldehyde and sucrose aldehyde cross-linked cationized gelatin nanofibrous mats

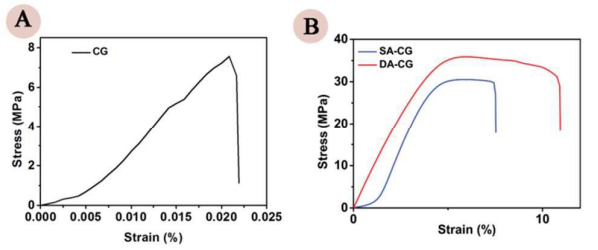

Figure 9: Stress – strain behaviour of CG nanofiber mats (A) Un cross-linked CG mat, (B) DA and SA cross-linked CG mats

Biological studies

Adhesion of L-929 fibroblast cells: Cross-linked CG nanofibers are evaluated for adhesion of L-929 fibroblast cells. The morphology of the fibroblast cells adhered on the DA-CG and SA-CG mats in comparison with control cover glass after 48 h of contact is shown in Figure 10. The results exhibit the suitability of both DA and SA as cross-linking agents for CG nanofibers. Fluorescent microscopic images of L-929 cells cultured on the cross-linked mats reveal that considerable amount of cells are grown on the DA-CG and SA-CG mats with well-distributed actin filament and nuclei. This cell attachment study clearly shows the efficiency of CG nanofibers cross-linked with the natural cross-linkers to promote cell adhesion.

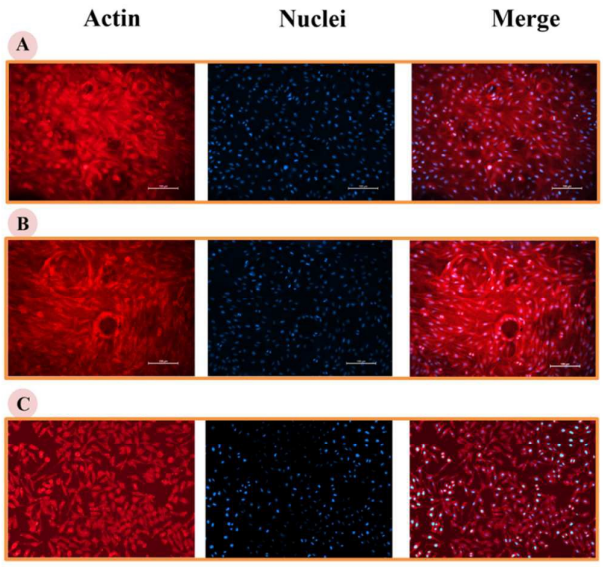

Figure 10: Fluorescent microscopic images of L-929 cells adhered on (A) dextran aldehyde-cationized gelatin mat, (B) sucrose aldehyde-cationized gelatin mat and (C) control cover glass after 48 h culture.

Adhesion, proliferation and viability of MG-63 osteoblast cells: Cell adhesion, viability, spreading and actin development of MG-63 cells cultured on CG nanofibrous mats are observed under confocal microscopy. The images taken on the fifth day of culture are shown in Figure 11 for actin morphology and Figure 12 for cell viability and growth. The cells grow abundantly on DA-CG and SA-CG mats with well distributed actin filaments and prominent nuclei. Most of the cells are observed to be viable on the mats. This indicates that DA-CG and SA-CG mats support the intracellular esterase activity of the cells. MG-63 osteoblast cell adhesion is a primary evaluation of the biomaterial to be used as bone tissue engineering scaffold. Electrospun scaffold made up of a variety of polymers are employed as bone tissue engineering matrix such as polycaprolactone (PCL) [32], polycaprolactone/nanohydroxyapetite/collagen (PCL/nHA/col) [33], gelatin/PCL [5] and others. Several collagen and gelatin based electrospun scaffolds are found to mimic bone microenvironment [34]. The nanofibrous architecture of CG mat also encourages osteoblast cell attachment due to the properties of nanofibers such as large surface area and improved surface functionality. This provides enhanced cell growth and better cell-material interactions. Moreover, the positive charges on the surface of CG nanofibers facilitate cell adhesion of different cells due to the interaction with negatively charged cell membranes.

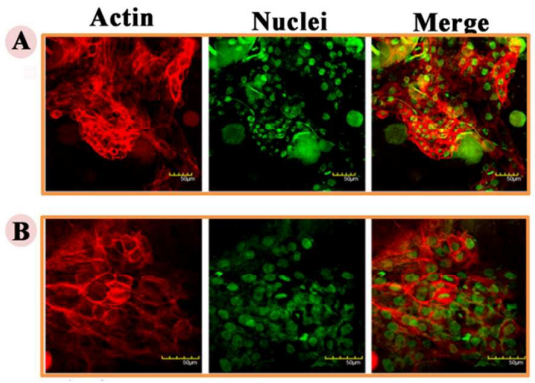

Figure 11: The confocal laser micrographs of human osteoblast cells (MG-63) on the cross-linked cationizedgelatin nanofibers stained with Rhodamine–phalloidin for actin filaments (red) and Hoechst 33342 for nuclei (green). The cells are cultured on cationized gelatin nanofibers cross-linked with (A) dextran aldehyde; (B) sucrose aldehyde.

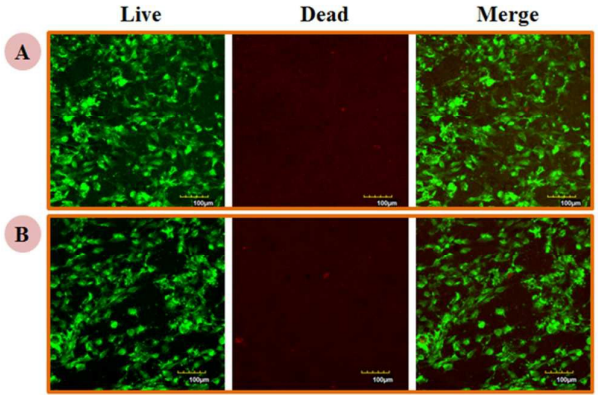

Figure 12: Fluorescence micrograph of the live and dead stained MG63 cells. The osteoblast like cells are grown on (A) dextran aldehyde, (B) sucrose aldehyde cross-linked cationized gelatin samples for 5 days. Calcein AM is used to stain live cells (green) and ethidiumhomodimer for dead cells (red). The cells are visualized using 488 and 543 lasers under confocal microscope. Scale bar represents 100 micron.

For assessing the cell proliferation of MG-63 osteoblast cells on the cross-linked CG nanofibers, Alamar blue assay is carried out. For comparison of the results, glutaraldehyde cross-linked CG nanofibers (GT-CG) are also evaluated for cell proliferation. Equal numbers of cells are seeded on the cross-linked CG mats. It is observed that cells grow normally on the mats for a period of 7 days. Till 5th day, there is not much growth rate observed for both of the samples. This time can be considered as the adaptation period for the cells to the new environment. A good growth rate can be observed for DA-CG and SA-CG samples from 5 to 7 days (Figure 13). The data at day 3, 5 and 7 are significantly different than the first day of cell seeding, which signifies ample cell growth on the day points. Cells are not proliferating on GT-CG mat during these periods, indicating the toxic response of residual glutaraldehyde.

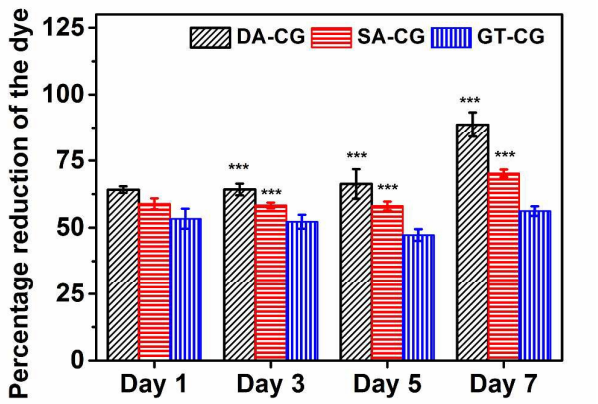

Figure 13: The cell attachment and proliferation on DA-CG, SA-CG and GT-CG nanofibers. Initial cell seeding density is 2000 cells/scaffold. Data represented as the mean ± standard error (***p≤0.001)

Osteoblasts cells are of mesenchymal origin and are mainly responsible for bone matrix synthesis and mineralization. They produce a collagen type I rich extracellular matrix in vivo [35]. It is well known that natural bone is a nanocomposite consisting of collagen fibers and hydroxyapatite (HAP). HAP is orderly deposited within nanofibrous collagen matrix [36]. Gelatin and its derivatives are alternatives for collagen. Hence, nanofibers based on gelatin and cationized gelatin may mimic the bone microenvironment. In this work, the surface bioactivity is improved by cationizing gelatin with an aim to improve the binding ability of osteoblast cells. In case of natural bone ECM, HAP has an important role, such as good osteoconductivity and bone binding ability [37]. For assisting the bone mineralization, the cationized gelatin can be mixed with HAP to achieve composite nanofibers. This may combine the mechanical strength and bone mineralization properties of HAP with cytocompatibility and cell adhesion properties of cationized gelatin. This study reports osteoblast cell attachment, proliferation and viability on the nanofibrous mats, which are the primary features required for bone tissue engineering. The results indicate that the cationized gelatin nanofibers may promote different types of bone regenerations especially for soft bones such as ear and nose. The CG nanofibers may also be potential matrices for other types of cells like keratinocytes for skin regeneration and chondrocytes for cartilage repair.

Conclusions

The chemical modification of gelatin via amination produces cationized gelatin. The modified gelatin is water soluble without forming gel at room temperature. This is the first report for nanofiber fabrication method using the cationized gelatin by means of pure water as the solvent. The fabricated nanofiber is cross-linked using natural and cost effective cross-linking agents. They are better alternatives for glutaraldehyde and genipin. The positive charge on the surface of nanofibers interacts with negatively charged cell surface,

making them an exciting class of materials for tissue regeneration. The modification of gelatin and its combination with novel cross-linkers demonstrate the versatility of this biomaterial. This ensures its role as a matrix for various tissue regenerations.

Acknowledgements

Authors are grateful to Director, IIST for financial support. Authors acknowledge Indian Institute of Technology (IIT Madras) for providing the SEM facility and Dr. T Pradeep (IIT Madras) for providing XPS facility. SCK's laboratory work is supported by Department of Biotechnology and Indian Council of Medical Research, Govt. of India.

References

1 Y. S. Choi, S. R. Hong, Y. M. Lee, K. W. Song, M. H. Park and Y. S. Nam, *Biomaterials*, 1999, **20**, 409-417.

2 L. Jeong and W. H. Park, *International journal of molecular sciences*, 2014, **15**, 6857-6879.

3 J. Padrão, J. P. Silva, L. R. Rodrigues, F. Dourado, S. Lanceros-Méndez and V. Sencadas, *Soft Materials*, 2014, **12**, 247-252.

4 N. Bhardwaj and S. C. Kundu, *Biotechnology Advances*, 2010, **28**, 325-347.

5 Z.-M. Huang, Y. Z. Zhang, S. Ramakrishna and C. T. Lim, *Polymer*, 2004, **45**, 5361-5368.

6 J. A. Matthews, G. E. Wnek, D. G. Simpson and G. L. Bowlin, *Biomacromolecules*, 2002, **3**, 232-238.

7 C. S. Ki, D. H. Baek, K. D. Gang, K. H. Lee, I. C. Um and Y. H. Park, *Polymer*, 2005, **46**, 5094-5102.

8 S. Panzavolta, M. Gioffrè, M. L. Focarete, C. Gualandi, L. Foroni and A. Bigi, *Acta biomaterialia*, 2011, **7**, 1702-1709.

9 M. Angarano, S. Schulz, M. Fabritius, R. Vogt, T. Steinberg, P. Tomakidi, C. Friedrich and R. Mülhaupt, *Adv. Funct. Mater.*, 2013, **23**, 3277-3285.

10 Y. Z. Zhang, J. Venugopal, Z. Huang, C. T. Lim and S. Ramakrishna, *Polymer*, 2006, **47**, 2911-2917.

11 M. Bertoldo, S. Bronco, T. Gragnoli and F. Ciardelli, *Macromol. Biosci.*, 2007, **7**, 328-338.

12 A. J. Kuijpers, G. H. Engbers, J. Krijgsveld, S. A. Zaat, J. Dankert and J. Feijen, *J. Biomater. Sci., Polym. Ed.*, 2000, **11**, 225-243.

13 Y. Hao, P. Xu, C. He, X. Yang, M. Huang, J. Xing and J. Chen, *Nanotechnology*, 2011, **22**, 285103.

14 W.-H. Chang, Y. Chang, P.-H. Lai and H.-W. Sung, *J. Biomater. Sci., Polym. Ed.*, 2003, **14**, 481-495.

15 K. Jalaja, P. R. A. Kumar, T. Dey, S. C. Kundu and N. R. James, *Carbohydr. Polym.*, 2014, **114**, 467-475.

16 K. Jalaja and N. R. James, *Int. J. Biol. Macromol.*, 2015, **73**, 270-278.

17 M. Gómez-Guillén, B. Giménez, M. a. López-Caballero and M. Montero, *Food Hydrocolloids*, 2011, **25**, 1813-1827.

18 J. Zhou, J. Liu, C. J. Cheng, T. R. Patel, C. E. Weller, J. M. Piepmeier, Z. Jiang and W. M. Saltzman, *Nat. Mater.*, 2012, **11**, 82-90.

19 S. K. Samal, M. Dash, S. Van Vlierberghe, D. L. Kaplan, E. Chiellini, C. van Blitterswijk, L. Moroni and P. Dubruel, *Chem. Soc. Rev.*, 2012, **41**, 7147-7194.

20 S. Gorgieva and V. Kokol, *Biomaterials Applications for Nanomedicine*, 2011, 17-58.

21 K. Morimoto, S. Chono, T. Kosai, T. Seki and Y. Tabata, *Drug Delivery*, 2008, **15**, 113-117.

22 J. Wang, Y. Tabata, D. Bi and K. Morimoto, *Journal of controlled release : official journal of the Controlled Release Society*, 2001, **73**, 223-231.

23 M. Santoro, A. M. Tatara and A. G. Mikos, *J. Controlled Release*, 2014, **190**, 210-218.

24 H. Fujii, A. Matsuyama, H. Komoda, M. Sasai, M. Suzuki, T. Asano, Y. Doki, M. Kirihata, K. Ono, Y. Tabata, Y. Kaneda, Y. Sawa and C. M. Lee, *Radiation oncology (London, England)*, 2011, **6**, 8-8.

25 J.-P. Chen and C.-H. Su, *Acta biomaterialia*, 2011, **7**, 234-243.

26 H. Shen, X. Hu, F. Yang, J. Bei and S. Wang, *Biomaterials*, 2007, **28**, 4219-4230.

27 Y. Lu, H. Jiang, K. Tu and L. Wang, *Acta Biomaterialia*, 2009, **5**, 1562-1574.

28 M. Sokolsky-Papkov, A. J. Domb and J. Golenser, *Biomacromolecules*, 2006, **7**, 1529-1535.

29 R. Schoevaart, A. Siebum, F. van Rantwijk, R. Sheldon and T. Kieboom, *Starch - Stärke*, 2005, **57**, 161-165.

30 C. M. Vaz, L. A. de Graaf, R. L. Reis and A. M. Cunha, *Polym. Degrad. Stab.*, 2003, **81**, 65-74.

31 L. Damink, P. Dijkstra, M. Van Luyn, P. Van Wachem, P. Nieuwenhuis and J. Feijen, *Biomaterials*, 1996, **17**, 679-684.

32 H. Yoshimoto, Y. M. Shin, H. Terai and J. P. Vacanti, 2003, **24**, 2077-2082.

33 J. Venugopal, S. Low, A. T. Choon and S. Ramakrishna, *Journal of Biomedical Materials Research Part B: Applied Biomaterials*, 2008, **84**, 34-48.

34 K. Sisson, C. Zhang, M. C. Farach-Carson, D. B. Chase and J. F. Rabolt, *Journal of Biomedical Materials Research Part A*, 2010, **94**, 1312-1320.

35 U. Kini and B. Nandeesh, in *Radionuclide and Hybrid Bone Imaging*, Springer, 2012, pp. 29-57.

36 C. He, F. Zhang, L. Cao, W. Feng, K. Qiu, Y. Zhang, H. Wang, X. Mo and J. Wang, *J. Mater. Chem.*, 2012, **22**, 2111-2119.

37 C. Klein, P. Patka, J. Wolke, J. de Blieck-Hogervorst and K. De Groot, *Biomaterials*, 1994, **15**, 146-150.

Journal Name

ARTICLE

Table of content only

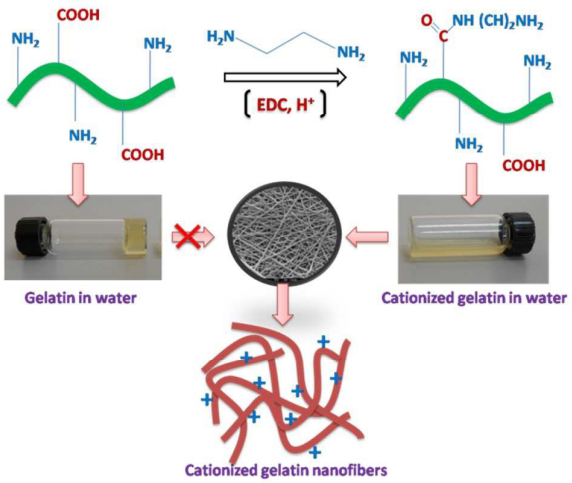

A green fabrication approach has been developed to produce biocompatible and non-cytotoxic cationically modified gelatin nanofibers with enhanced biological performance